International Journal of Innovative
Computing, Information and Control
Volume **12**, Number **3**, June **2016**

 ISSN 1349-4198
pp. 899–914

SYNCHRONIZATION ANALYSIS OF A PRODUCTION PROCESS UTILIZING STOCHASTIC RESONANCE

Kenji Shirai[1] and Yoshinori Amano[2]

[1]Faculty of Information Culture
Niigata University of International and Information Studies
3-1-1, Mizukino, Nishi-ku, Niigata 950-2292, Japan
shirai@nuis.ac.jp

[2]Kyohnan Elecs Co., LTD.
8-48-2, Fukakusanishiura-cho, Fushimi-ku, Kyoto 612-0029, Japan
y_amano@kyohnan-elecs.co.jp

Received October 2015; revised March 2016

Abstract. *We report a stochastic resonance phenomenon in production processes. Intervention by outside companies and workers (internal force) is treated as an input noise (stochastic element) to successive processes in the production system. We assume self-similarity in this system. By varying two of the system parameters (external and internal forces), we reveal an optimal combination of the throughput threshold for evaluating the working process and the magnitude of volatility (noise intensity) in a worker's ability. Moreover, because of this optimal combination, a stochastic resonance occurs in this system. The existence of stochastic resonance is confirmed in the actual data of a production flow system. The results of this study can assist the development of market-driven, innovative production companies.*

Keywords: Stochastic resonance, Self-similarity, Power spectral density, Lead time, Production process

1. **Introduction.** Based on mathematical and physical understanding of production engineering, we are conducting research aimed at establishing an academic area called mathematical production engineering. As our business size is a small-to-medium-sized enterprise, human intervention constitutes a significant part of the production process, and revenue can sometimes be greatly affected by human behavior. Therefore, when considering human intervention from outside companies, a deep analysis of the production process and human collaboration is necessary to understand the potential negative effects of such intervention.

With respect to mathematical modeling of deterministic systems, a physical model of the production process was constructed using a one-dimensional diffusion equation in 2012 [1]. However, many concerns that occur in the supply chain are major problems facing production efficiency and business profitability. A stochastic partial bilinear differential equation with time delay was derived for outlet processes. The supply chain was modeled by considering as time delay [3]. With respect to the analysis of production processes in stochastic systems based on financial engineering, we have proposed that a production throughput rate can be estimated utilizing a Kalman filter based on a stochastic differential equation [2]. We have also proposed a stochastic differential equation (SDE) for the mathematical model describing production processes from the input of materials to the end. We utilized a risk-neutral principal in stochastic calculus based on the SDE [4].

With respect to the analysis of production processes based on physics, we have clarified that phenomena such as power-law distributions, self-similarity, phase transitions, and

on-off intermittency can occur in production processes [5, 6, 7, 8, 9]. On the other hand, there is the famous theory of constraints (TOC) that describes the importance of avoiding bottlenecks in production processes [10]. Small fluctuations in an upstream subsystem appear as large fluctuations in the downstream (the so-called bullwhip effect) [13]. The bullwhip effect generates a large gap between the demand forecasts of the market and suppliers. Large fluctuations can be suppressed by the following mechanisms.

(1) Reducing the lead time, improving the throughput, and synchronizing the production process by the TOC.
(2) Sharing the demand information and performing mathematical evaluations.
(3) Analyzing the reduction and fluctuating demands of the subsystem (using nonlinear vibration theory).
(4) Basing the inventory management approach on stochastic demand.

When using manufacturing equipment, delays in one production step are propagated to the next. Hence, the use of manufacturing equipment itself may lead to delays. The improvement of production processes was presented that the "Synchronization with pre-process" method was the most desirable in practice using the actual data in production flow process based on the cash flow model by using the SDE of log-normal type [11]. In essence, we have proposed the best way, which is a synchronous method using the Vasicek model for mathematical finance [12]. Then, the supply chain theme, which was a time delay in the production processes, was proposed for the throughput improvement based on a stochastic differential equation of log-normal type [13].

Moreover, the analysis of the synchronized state indicated that this state was a much better method from the viewpoint of potential energy [13, 14]. We have also shown that the phase difference between stages in a process corresponded to the standard deviation of the working time [16]. When the phase difference was constant, the total throughput could be minimized. We showed that a synchronous process could be realized by the gradient system. The above problem is not limited to small- and medium-sized companies; in all cases, human interventions that directly affect the production process present a major challenge.

In general, we may reasonably consider that human interventions within and outside of the production system (internal and external forces, respectively) introduce uncertainties into the system's progress [4, 12]. The production system is formed by connecting both elements. When human intervention from outside companies involves an uncertainty, the noise element is frequently overlooked; instead, researchers have focused on efficient production or manufacturing the best system. Moreover, by including the noise element, we can recognize the unique advantage of the system. We consider internal and external forces as two parameters in the production system. Rather than selecting the ratio between lead time and throughput that optimizes an individual's productivity, we select the parameters that achieve overall synchronization [4, 12]. In our previous study of a production system involving worker intervention, the specific abilities of workers required empirical analysis. To optimize typical modern production systems, we must recognize the importance of biological fluctuations. For example, the following aims typify technical innovation in the engineering industries:

(1) Detecting a small signal using the noise in the force.
(2) Synchronizing the circuit groups using the noise power.

Stochastic resonance (SR) is utilized in physical systems such as electronic circuits, and even in biological systems such as neurotransmission; as a result, the same phenomenon has been confirmed [18, 19]. However, there have been no reports on application of SR

in production processes for the improvement of throughput. Accordingly, we present the improvement of throughput in production processes using SR in the present study.

In this study, worker productivity in a high-mix, low-volume production process is optimized for the market demand, rather than the mass production process. To demonstrate the effectiveness of the throughput when the worker productivity is analyzed in this manner, we extract the probability distribution of the productivities of workers in a real production firm. Analyzing the actual results, we ascertain the probabilities of human factors in a production process.

Fujisaka and colleagues modeled the production process as a circuit system with an annular structure and coupled synchronization loops [20]. A production flow process used in our actual processes is regarded as the coupled synchronization loops reported in Fujisaka's reference [20]. Here, we apply their model to a relatively simple cascaded system, and model the dynamics using their derived Fokker-Planck equation (FPE). The FPE applies the modulation content of the equilibrium solution to the operator as the stochastic variation, and seeks the response and correlation functions. In their numerical calculations, Fujisaka and colleagues obtained the output signal-to-noise ratio, but did not calculate the eigenvalues and eigenfunctions of the operators in the fluctuating solution.

As described above, we consider that the noise (stochastic component) in workers' capability follows a probability distribution. We study the relationship between the intensity of SR (volatility in workers' ability) and the throughput (lead time) by capturing the process as a type of threshold reaction element. The proposed concept can potentially lead to innovative productivity by companies implementing a production system. Although the test system is small, it contains useful data for analyzing an innovative production system.

2. Mathematical Modeling of Production Processes.

2.1. Production systems in the production equipment industry.

The production methods used in equipment are briefly covered in this paper (refer to Figure 1). Please see our research [5]. This system is considered to be a 'Make-to-order system with version control', which enables manufacturing after orders are received from clients, resulting in 'volatility' according to its delivery date and lead time. In addition, there is volatility in the lead time, depending on the content of the make-to-order products (production equipment).

2.2. Production flow process.

A manufacturing process that is termed as a production flow process is shown in Figure 2. The production flow process, which manufactures low volumes of a wide variety of products, is produced through several stages in the production process. In Figure 2, the process consists of six stages. In each step S1-S6 of the manufacturing process, materials are being produced.

The direction of the arrows represents the direction of the production flow. Production materials are supplied through the inlet and the end-product is shipped from the outlet [11].

2.3. Concept of production flow.

We have reported a mathematical model of the production process in the past manuscripts. We describe the physical approach for a production process [1, 2]. From Figure 3, we refer to the network ability (i.e., a statically acceptable amount of production) in an interprocess network (a production field) as R. An interprocess network indicates a sequential flow from one process to the other after the completion of the current process. Here assuming that the production density function

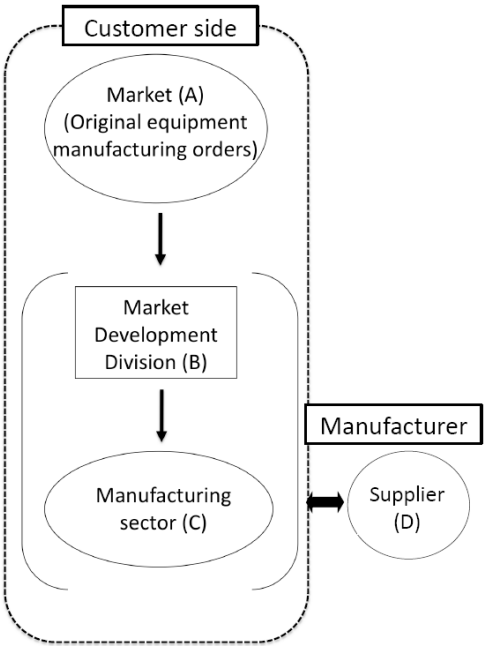

FIGURE 1. Business structure of company of research target

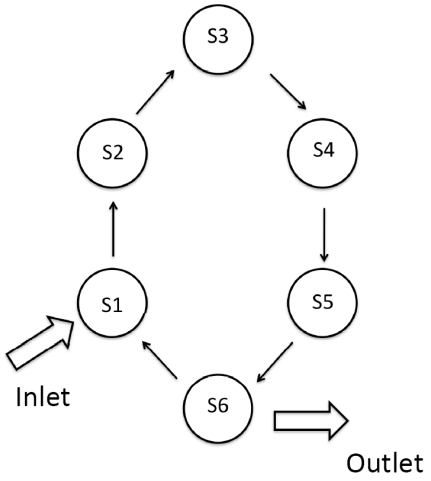

FIGURE 2. Production flow process

for the i-th equipment is $S_i(x,t)$, $S_i(x,t)$ is expressed by

$$[J(x,t)dt - J(x+dx,t)dt]R = [S_i(x,t+dt) - S_i(x,t)]Rdx \tag{1}$$

where J is the production flow [1].

Next, we define the production flow as the displacement of a production density function in the unit production direction. In other words, the production density function is proportional to the cost necessary for production, and thus, it can be considered as the production cost per unit production. Furthermore, because production leads to a return, the production density function can be considered as a return density function

$$\frac{\partial S_i(x,t)}{\partial t} = D\frac{\partial^2 S_i(x,t)}{\partial x^2} \tag{2}$$

where D is the diffusion coefficient, t is the time variable, and x is the spatial variable.

This equation is equivalent to the diffusion equation derived from the minimization condition of free energy in a production field, indicating that the connections between processes can be treated as a diffusive propagation of products (refer to Figure 3) [1].

A model of the production process, which is connected in one dimension, is described in Figure 3. The process of production is indicated by the movement of production units from one process (node) to another. This production flow is equivalent to transmission rate, which is defined as the rate of data flow between connected nodes in communication engineering. Accordingly, we formulate the production model in a manner similar to heat propagation in physics. Thus, the production process is modeled mathematically using a continuous diffusion type of partial differential equation consisting of time and spatial variables [1].

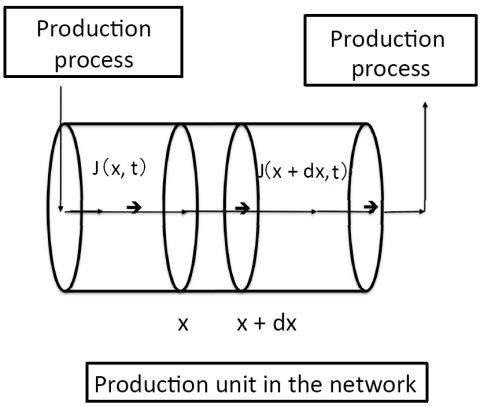

FIGURE 3. Network inter-process division of the worker

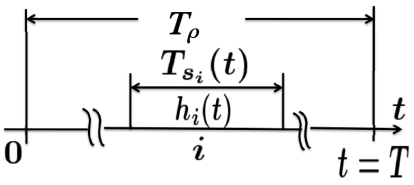

FIGURE 4. Conceptual model of the process cycle period and duration

3. Spectral Values Considering Stochastic Resonance.

3.1. **Spectrum analysis of throughput deviations within a process.** In our previous study, we confirmed that the throughput deviations for manufacturing equipment are properly predicted by a dynamic model based on a Langevin equation [5, 14, 21]. The spectrum analysis is detailed in our previous study with respect to the throughput deviation within a process [6].

Regarding the periodic cycle, we define a cycle of period i as $T_{s_i}(t)$ and $T_\rho(t)$ as the cycle until the end of the company's fiscal year. In Figure 4, $T_{s_i}(t)$ indicates a cycle of period i and $T_\rho(t)$ represents a company's fiscal year. Then, the relationship between $T_{s_i}(t)$ and $T_\rho(t)$ is expressed as follows.

$$T_{s_i}(t) = \frac{1}{h_n(t)} \tag{3}$$

When $T_\rho(t) \equiv f_{req}$, we refer to f_{req} as the company's period frequency.

Then, from the Wiener-Khinchin theorem, a power spectrum $S_{h_n}(f_{req})$ of $h_n(t)$ to f_{req} is expressed by the following [23].

$$S_{h_n}(f_{req}) \cong \int_0^\infty \cos(2\pi f_\rho \cdot t)\phi_{h_n}(t)dt \tag{4}$$

$$\phi_\tau(t) \cong \int_0^\infty \cos(2\pi f_{req} \cdot t)S_{h_n}(f_{req})df_{req} \tag{5}$$

Then we obtain as follows:

$$S_{h_n}(f_\tau) \approx D_f < |h_n|^2 > \tag{6}$$

Here if a time constant exists in the time correlation function of fluctuation, we can derive the following [23].

$$\phi_{h_n}(t) = D_f < |h_i|^2 > \cdot \exp\Big(-\frac{t}{\tau_n}\Big) \tag{7}$$

Then, we substitute Equation (7) into Equation (4) for $S_{h_n}(f_{req})$. Thus, we can obtain the following after calculating Equation (4). Please see a more detailed analysis in our previous study [6].

$$S_{h_n}(f_{req}) =< |h_n|^2 > \cdot \frac{D_f\tau_n}{(2\pi f_{req}\tau_n)^2 + 1} \tag{8}$$

From Equation (8), we observe that Equation (6) represents the spectral correlation function of throughput deviation, whose Lorentz spectrum lies near the fluctuation frequency. Therefore, the spectrum is calculated from the defined throughput.

3.2. **Theoretical equation of SNR.** We assume that noise is added to the operator; that is, we assume volatility in the data of the production flow system, which are applied as the input signal. The SNR is computed from the power spectral density of the noise intensity and the throughput deviation. The result confirms the presence of stochastic resonance in the production process. Here the noise intensity represents the volatility in the worker ability.

Definition 3.1. *Theoretical equation of SNR*

$$SNR \equiv \left[\frac{T_s \cdot < S_{h_n}(f_{req}) >}{S_N}\right]^2 \cdot \exp\Big(-\frac{T_s}{S_N}\Big) \tag{9}$$

where $f_{req} \approx 1/T_s$ and T_s is a cycle time, and S_N is a power spectral density of noise and S_N is proportional to a volatility.

The SNR of the production flow process is

$$SNR \equiv \frac{< S_{h_n}(f_{req}) >}{S_N} \tag{10}$$

4. Numerical Simulation.

4.1. **Calculation of SNR.** The evaluation of theoretical equation (Equation (9)) and approximation equation (Equation (10)) are represented as follows.

(1) According to the time constant (τ) of autocorrelation function increases, the spectral peak value is shifted to the left (see Figures 5-8, Figures 9-12, Table 1 and Table 2). There are so many situations that are over the standard working time; it is corresponding to Figure 5/Figure 6, Figure 9/Figure 10, Figure 13/Figure 14 and Table 4 that is an asynchronous process (test run 1). A synchronous process (test run 2, 3) indicates Figure 7/Figure 8, Figure 11/Figure 12, Figure 15/Figure 16 and Table 6/Table 8. In other word, the stochastic resonance occurs in Figure 7/Figure 8, Figure 11/Figure 12, Figure 15/Figure 16 and Table 6/Table 8.
(2) The value of SNR is the larger at near $T_s \approx 17$ or 20 from our theory and makes greater at $T_s \leq 20$.

We confirmed stochastic resonance in a test run of a production flow system. The threshold was set to $T_s \approx 20$.

Stochastic resonance can occur by the following mechanism. First, if the threshold is varied, the noise intensity amplifies in response to the large uncertainties in the overall system and in human factors. Consequently, the thresholds are always exceeded and stochastic resonance is not observed. However, stochastic resonance emerges when each process is assigned the same threshold $T_s \approx 20$. The threshold response pulses that

TABLE 1. Transition of noise intensity peak value on stochastic resonance (Equation (9))

Figure number	Time constant value τ	SNR value	Noise intensity
Figure 5	$\tau = 0.5$	9	8.85
Figure 6	$\tau = 1.0$	27	8.8
Figure 7	$\tau = 2.0$	57	7.85
Figure 8	$\tau = 3.0$	63	7.8

TABLE 2. Transition of noise intensity peak value on stochastic resonance of the production flow process (Equation (10))

Figure number	Time constant value τ	SNR value	Noise intensity
Figure 9	$\tau = 0.5$	0.08	28.6
Figure 10	$\tau = 1.0$	0.08	21.4
Figure 11	$\tau = 2.0$	0.08	8.3
Figure 12	$\tau = 3.0$	0.08	5.7

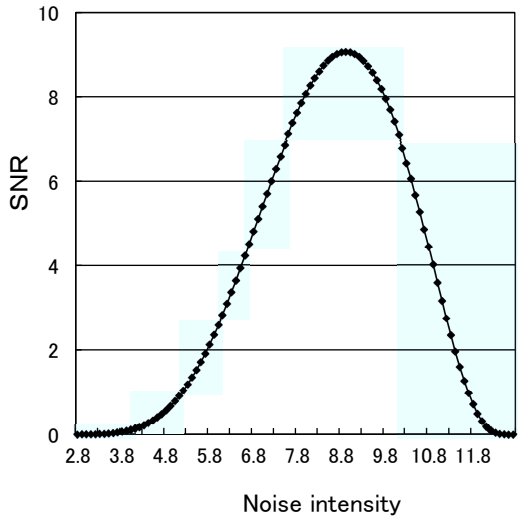

FIGURE 5. Stochastic resonance (Equation (9)), $D_\rho = 1$, $\tau = 0.5$, $T_s = 12.2$

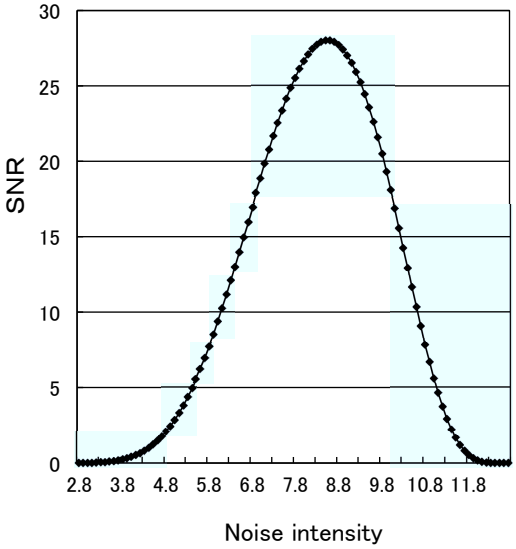

FIGURE 6. Stochastic resonance (Equation (9)), $D_\rho = 1$, $\tau = 1$, $T_s = 14$

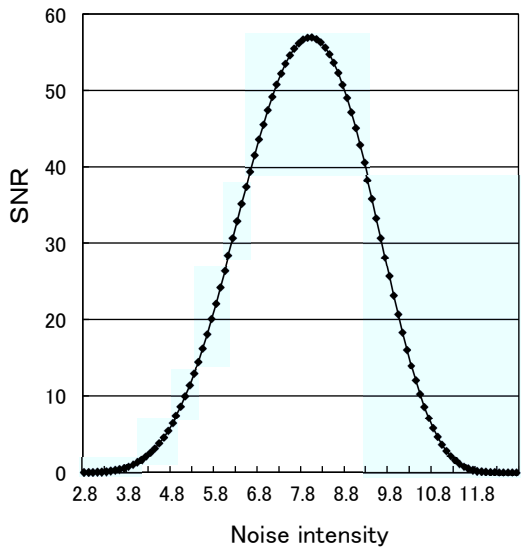

FIGURE 7. Stochastic resonance (Equation (9)), $D_\rho = 1$, $\tau = 2$, $T_s = 17.0$

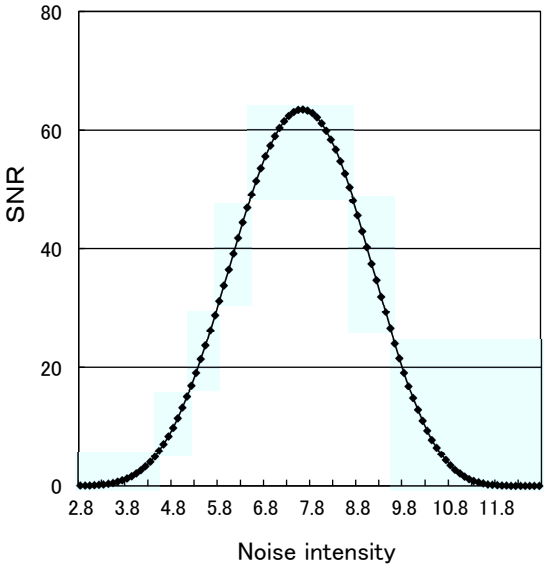

FIGURE 8. Stochastic resonance (Equation (9)), $D_\rho = 1$, $\tau = 3$, $T_s = 20$

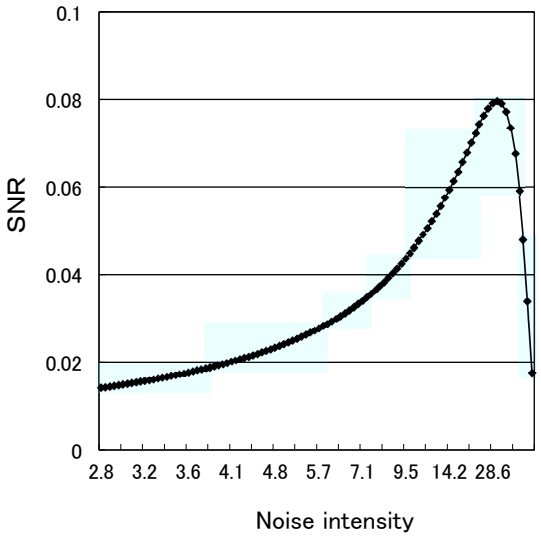

FIGURE 9. Stochastic resonance (Equation (10)), $D_\rho = 1$, $\tau = 0.5$

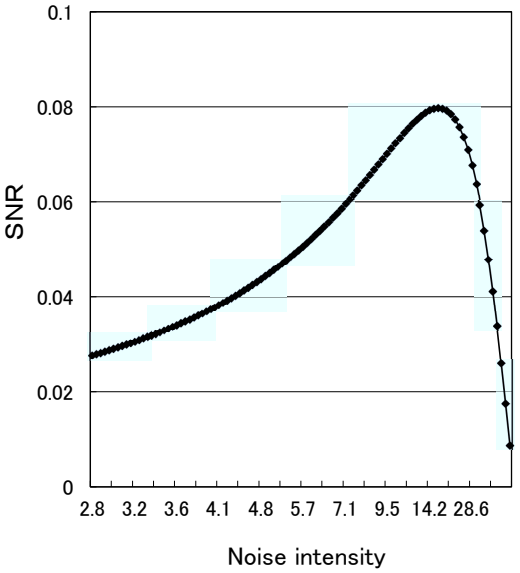

FIGURE 10. Stochastic resonance (Equation (10)), $D_\rho = 1$, $\tau = 1$

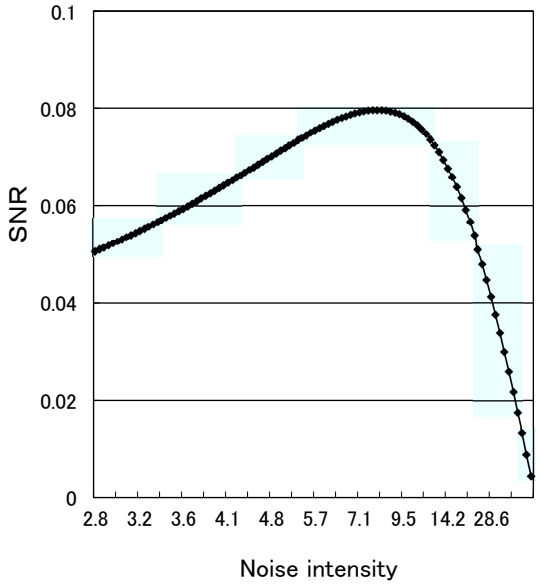

FIGURE 11. Stochastic resonance (Equation (10)), $D_\rho = 1$, $\tau = 2$

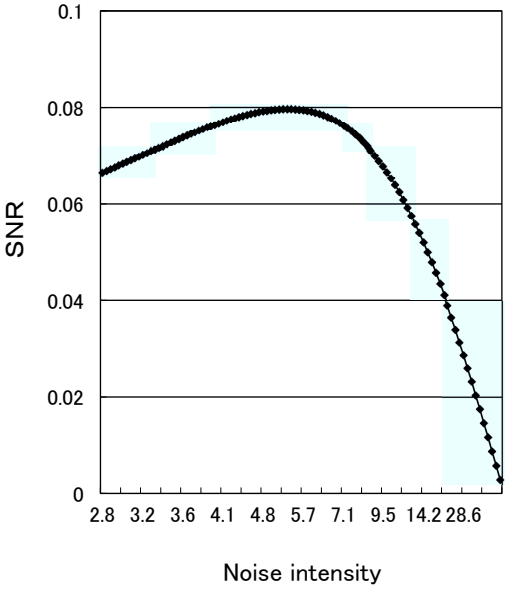

FIGURE 12. Stochastic resonance (Equation (10)), $D_\rho = 1$, $\tau = 3$

generate stochastic resonance are enclosed in the round-cornered boxes in Tables 4, 6, and 8. Thus, the more volatility is large, it is added a number circle. Test run 1 is larger than test run 2 and test run 3 in actual data. Please see the reference with respect to the actual data. [11, 17].

4.2. **Numerical simulation of spectral density Equation (8).** Frequency represents lead time; it is important to determine frequency. For example, Figures 13-16 show numerical examples of power spectral density versus frequency and represent the magnitude

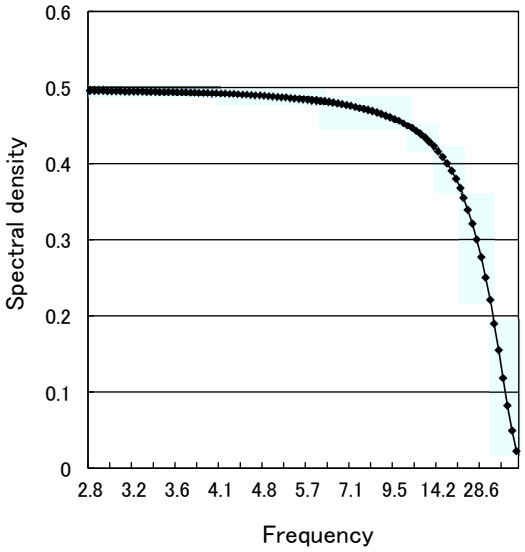

FIGURE 13. Spectral density of throughput deviation, $D_\rho = 1$, $\tau = 0.5$

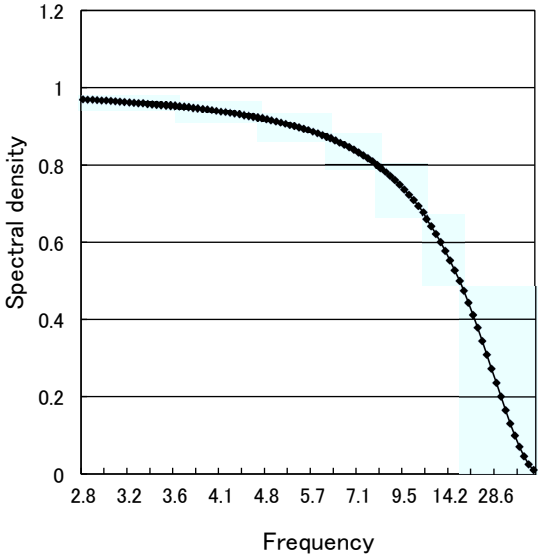

FIGURE 14. Spectral density of throughput deviation, $D_\rho = 1$, $\tau = 1$

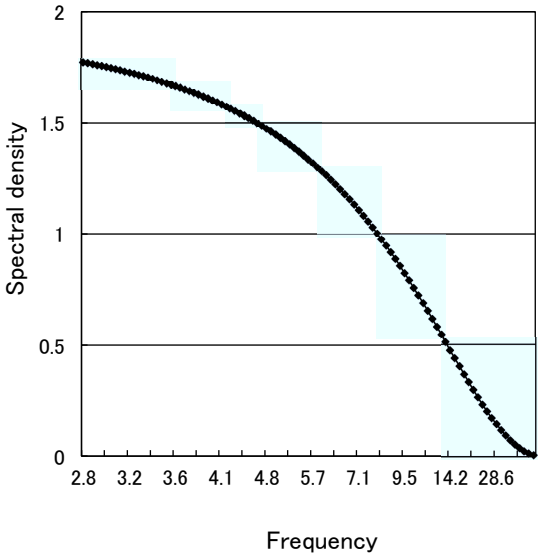

FIGURE 15. Spectral density of throughput deviation, $D_\rho = 1$, $\tau = 2$

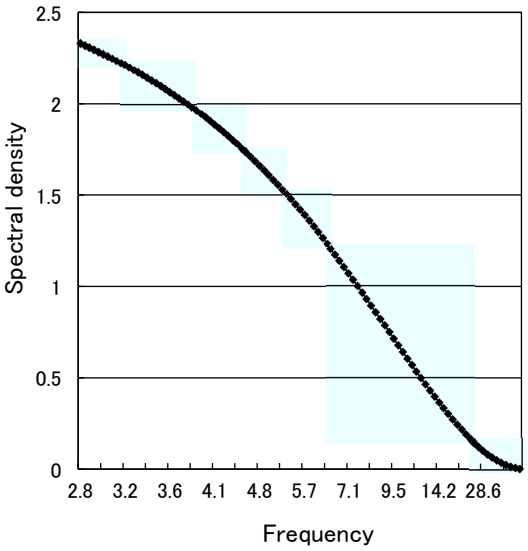

FIGURE 16. Spectral density of throughput deviation, $D_\rho = 1$, $\tau = 3$

of throughput deviations within a process at a certain range of frequencies. The similarity of the graph shapes, which show power spectral densities at a certain frequency ranges, also indicates self-similarity in the processes. Please see the reference [16].

By setting a certain range of frequencies, i.e., setting a target lead time, spectral density is maintained as low as possible. In other words, throughput deviations within a process are maintained as low as possible.

By maintaining high-throughput deviations within a process in the production system, a company produces high benefits.

TABLE 3. Correspondence between the test – run number

	Production process	Working time	Volatility
test run 1	Asynchronous process	627(min)	0.29
test run 2	Synchronous process	500(min)	0.06
test run 3	"Synchronization with preprocess" method	470(min)	0.03

4.3. **Calculation of potential function.** The phase difference $|\theta|$ is modulated by the fundamental period T_0, mostly likely because the internal system and worker abilities are stochastically disturbed (see Figure 17). Therefore, the basic process potential is acted upon by external forces, as indicated in the following equation.

$$V(\theta) = \sigma \cdot \theta + B(-4C\cos\theta + \cos 2\theta) \tag{11}$$

where σ is a volatility having an internal cause and disturbance. The σ is also the volatility of a stochastic throughput $C(x,t)(C(t))$.

Then, $\sigma \approx K_\sigma$, and K_σ is a real number. Therefore, Equation (11) is deformed as

$$V(\theta) = K_\sigma \cdot \theta + B(-4C\cos\theta + \cos 2\theta) \tag{12}$$

For example, we determined $K_\sigma \approx 0.29$ in test run 1, $K_\sigma \approx 0.06$ in test run 2 and $K_\sigma \approx 0.03$ in test run 3.

As clarified in the above calculations, the basic potential displaces by an amount that depends on K_σ. Moreover, the direction of the deviation depends upon the sign of K_σ. In the test run of the production flow system, importing the volatility as an uncertainty also affected the worker lead time. Thus, the coefficient of the external force partially represents the running capability of a process.

In future work, we will investigate the practical meaning of the parameters $\{B, C\}$. If these parameters are defined, we can specify the deviation (phase) of the potential function from its set value, and thereby describe a fluctuating process in detail. Consequently, we could mathematically model a production process and determine the threshold of the lead time (throughput) in stochastic resonance.

Using the potential function, we now evaluate the variation statuses of workers at different stages. In the numerical equations we adopt Equation (13), which includes a

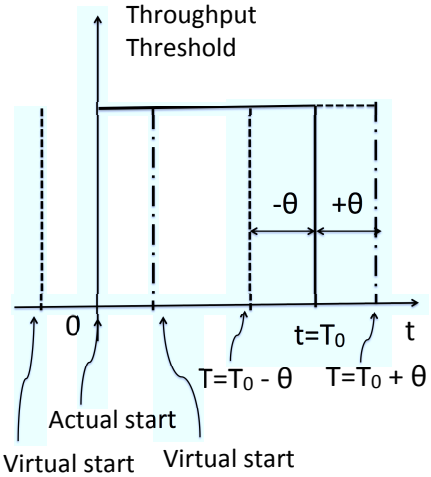

FIGURE 17. Stochastic resonance phenomenon

constant term F. Figures 18-25 plot the potential functions for different values of F, B, and C. Please see the references with respect to the graphs [16]. We find that if $|F| \geq 3\sqrt{3}B$, the process cannot be synchronized [22]. As shown in Figures 18-25, setting $F = 0.01$ does not affect the shape of the potential function, but setting $F = 0.2$ distorts the potential function and destroys its symmetry. In other words, when B is large, the production process cannot maintain synchronicity. In contrast, the potential function is insensitive to the parameters B and C, although reducing, i.e., C to 0.01 shortens the stabilization period.

$$V_F = F \times D + B \times (-4 \times C\cos(D) + \cos(2D)) \tag{13}$$

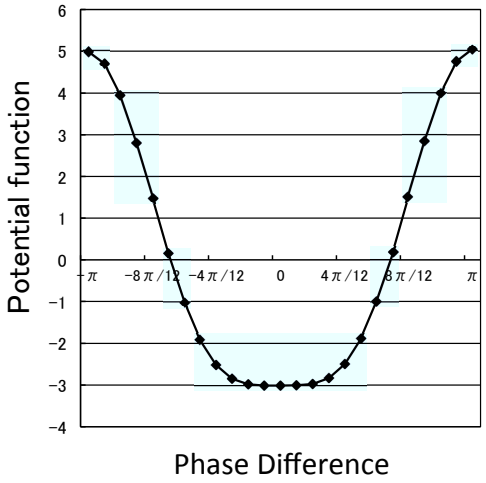

FIGURE 18. Value of potential function ($F = 0.01$, $B = 1$, $C = 1.5$)

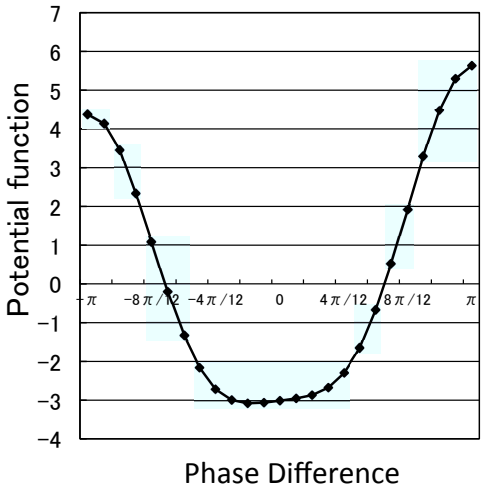

FIGURE 19. Value of potential function ($F = 0.2$, $B = 1$, $C = 1.5$)

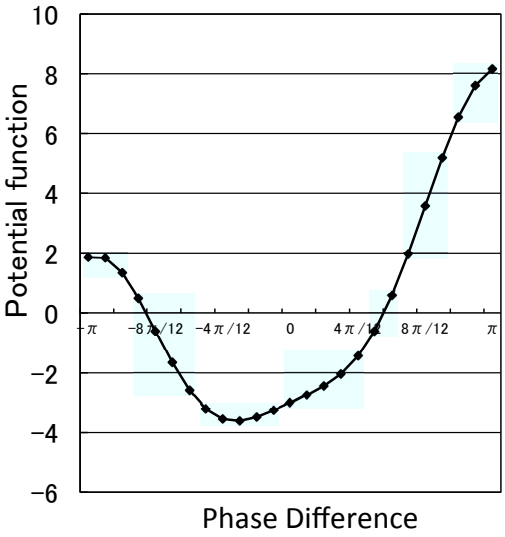

FIGURE 20. Value of potential function ($F = 1$, $B = 1$, $C = 1.5$)

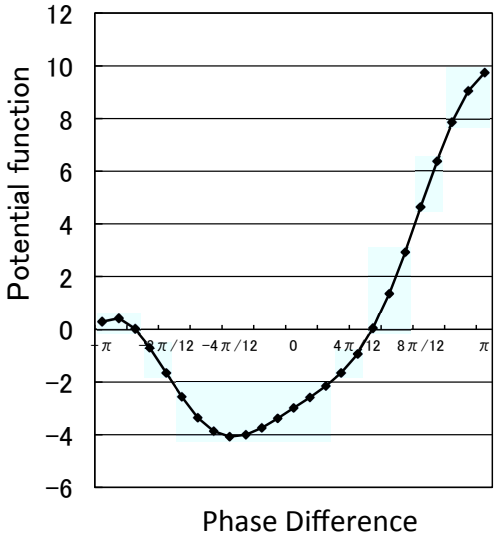

FIGURE 21. Value of potential function ($F = 1.5$, $B = 1$, $C = 1.5$)

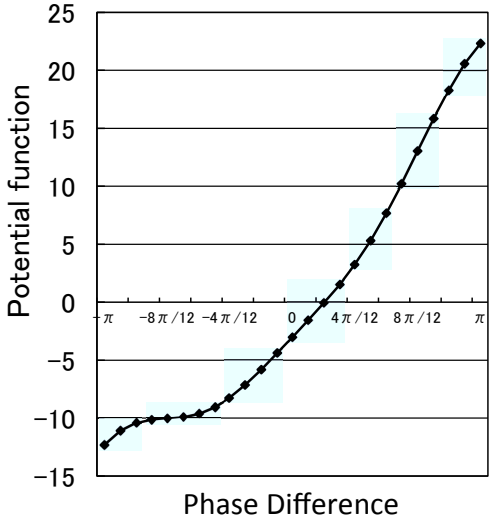

FIGURE 22. Value of potential function ($F = 5.5$, $B = 1$, $C = 1.5$)

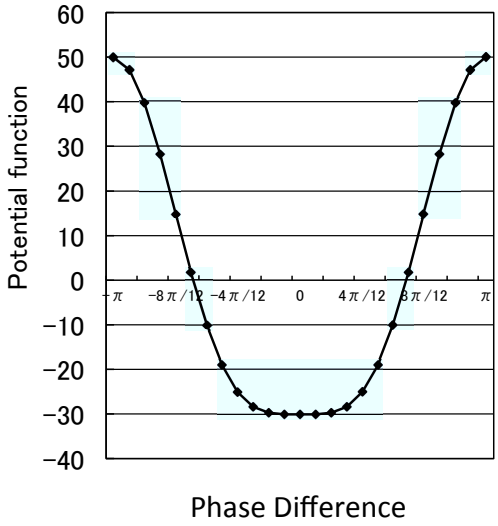

FIGURE 23. Value of potential function ($F = 0.01$, $B = 10$, $C = 1.5$)

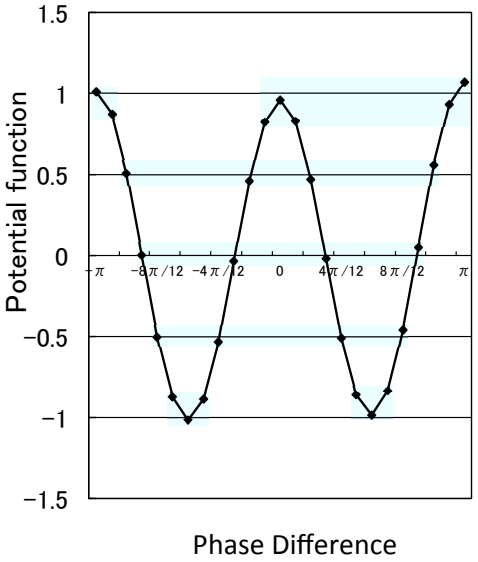

FIGURE 24. Value of potential function ($F = 0.01$, $B = 1$, $C = 0.01$)

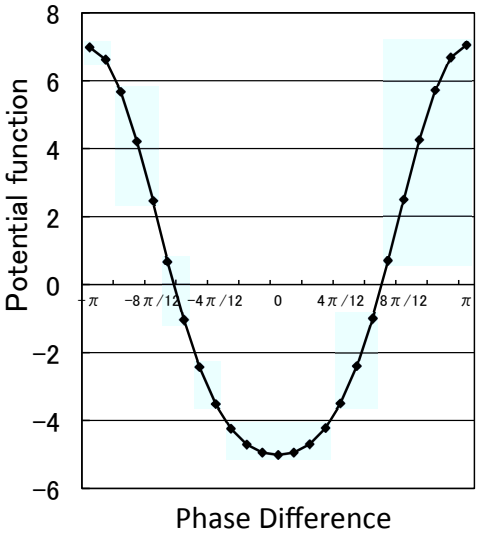

FIGURE 25. Value of potential function ($F = 0.01$, $B = 1$, $C = 1.5$)

5. **Conclusion.** Assuming self-similarity of the production system, we presented a theoretical analysis that is extendible to other production systems. The effectiveness of our model was validated using data from a real production flow, using suitable values of the parameters. In particular, we found a correlation between the magnitude of volatility in the distribution of worker abilities (noise intensity) and the threshold of the throughput decision (step throughput). We also found an optimal combination of these factors that was accompanied by stochastic resonance.

The developed equation models the throughput between mutual processes. The self-similarity of the model implies that downstream processes will follow the upstream model. We confirmed the presence of stochastic resonance from the SNR, obtained by relating

the background noise to the power spectral density. In future studies, we will increase the number of processes, and investigate their dynamics in a mutual-process model.

REFERENCES

[1] K. Shirai and Y. Amano, Prduction density diffusion equation and production, *IEEJ Trans. Electronics, Information and Systems*, vol.132-C, no.6, pp.983-990, 2012.

[2] K. Shirai and Y. Amano, A study on mathematical analysis of manufacturing lead time – Application for deadline scheduling in manufacturing system, *IEEJ Trans. Electronics, Information and Systems*, vol.132-C, no.12, pp.1973-1981, 2012.

[3] K. Shirai and Y. Amano, Model of production system with time delay using stochastic bilinear equation, *Asian Journal of Management Science and Applications*, vol.1, no.1, pp.83-103, 2015.

[4] K. Shirai, Y. Amano and S. Omatu, Process throughput analysis for manufacturing process under incomplete information based on physical approach, *International Journal of Innovative Computing, Information and Control*, vol.9, no.11, pp.4431-4445, 2013.

[5] K. Shirai, Y. Amano, S. Omatu and E. Chikayama, Power-law distribution of rate-of-return deviation and evaluation of cash flow in a control equipment manufacturing company, *International Journal of Innovative Computing, Information and Control*, vol.9, no.3, pp.1095-1112, 2013.

[6] K. Shirai and Y. Amano, Self-similarity of fluctuations for throughput deviations within a production process, *International Journal of Innovative Computing, Information and Control*, vol.10, no.3, pp.1001-1016, 2014.

[7] K. Shirai, Y. Amano and S. Omatu, Consideration of phase transition mechanisms during production in manufacturing processes, *International Journal of Innovative Computing, Information and Control*, vol.9, no.9, pp.3611-3626, 2013.

[8] K. Shirai and Y. Amano, Calculating phase transition widths in production flow processes using an average regression model, *International Journal of Innovative Computing, Information and Control*, vol.11, no.3, pp.1075-1091, 2015.

[9] K. Shirai and Y. Amano, On-off intermittency management for production process improvement, *International Journal of Innovative Computing, Information and Control*, vol.11, no.3, pp.1075-1092, 2015.

[10] S. J. Baderstone and V. J. Mabin, A review Goldratt's theory of constraints (TOC) – Lessons from the international literature, *Operations Research Society of New Zealand the 33rd Annual Conference*, University of Auckland, New Zealand, 1998.

[11] K. Shirai, Y. Amano and S. Omatu, Improving throughput by considering the production process, *International Journal of Innovative Computing, Information and Control*, vol.9, no.12, pp.4917-4930, 2013.

[12] K. Shirai and Y. Amano, Production throughput evaluation using the vasicek model, *International Journal of Innovative Computing, Information and Control*, vol.11, no.1, pp.1-17, 2015.

[13] K. Shirai, Y. Amano and S. Omatu, Propagation of working-time delay in production, *International Journal of Innovative Computing, Information and Control*, vol.10, no.1, pp.169-182, 2014.

[14] K. Shirai and Y. Amano, Application of an autonomous distributed system to the production process, *International Journal of Innovative Computing, Information and Control*, vol.10, no.4, pp.1247-1265, 2014.

[15] K. Shirai and Y. Amano, Throughput improvement strategy for nonlinear characteristics in the production processes, *International Journal of Innovative Computing, Information and Control*, vol.10, no.6, pp.1983-1997, 2014.

[16] K. Shirai and Y. Amano, Validity of production flow determined by the phase difference in the gradient system of an autonomous decentralized system, *International Journal of Innovative Computing, Information and Control*, vol.10, no.5, pp.1727-1745, 2014.

[17] K. Shirai and Y. Amano, Analysis of production processes using a lead-time function, *International Journal of Innovative Computing, Information and Control*, vol.12, no.1, pp.125-138, 2016.

[18] R. Benzi, A. Sutera and A. Vulpiani, The mechanism of stochastic resonance, *Journal of Physics A: Mathematical and General*, vol.14, no.11, pp.453-457, 1981.

[19] S. Ishiwata and K. Koizumi, Weak signal detection and its applications by stochastic resonance, *Phenomena and Mathematical Theory of Nonlinear Waves and Nonlinear Dynamical Systems*, Reports of RIAM Symposium No. 17ME-S2, 2005.

[20] H. Fujisaka, T. Kamio and K. Ikuiwa, Stochastic resonance in coupled sychronization loops, *IEICE*, vol.J90-A, no.11, pp.806-816, 2007.

[21] A. A. Stanislavsky, Fractional dynamics from the ordinary Langevin equation, *Physical Review, E 67*, pp.021111-1-021111-6, 2003.
[22] M. Sugi, H. Yuasa and T. Arai, Autonomous decentralized control of traffic signal network by reaction-diffusion equations on a graph, *Journal of SICE*, vol.39, no.1, pp.51-58, 2003.
[23] K. Kitahara, *Nonequilibrium Statistical Mechanics*, Iwanami Co., LTD, 2000.

Appendix A. **Analysis of Actual Data in the Production Flow System.** Figure 2 represents a manufacturing process called a flow production system, which is a manufacturing method employed in the production of control equipment. The flow production system, which in this case has six stages, is commercialized by the production of material in steps S1-S6 of the manufacturing process.

The direction of the arrow represents the direction of the production flow. In this system, production materials are supplied from the inlet and the end product will be shipped from the outlet.

Assumption A.1. *The production structure is nonlinear.*

Assumption A.2. *The production structure is a closed structure; that is, the production is driven by a cyclic system (production flow system).*

Assumption A.1 indicates that the determination of the production structure is considered as a major factor, which includes the generation value of production or the throughput generation structure in a stochastic manufacturing process (hereafter called the manufacturing field). Because such a structure is at least dependent on the demand, it is considered to have a nonlinear structure.

Because the value of such a product depends on the throughput, its production structure is nonlinear. Therefore, Assumption A.1 reflects the realistic production structure and is somewhat valid. Assumption A.2 is completed in each step and flows from the next step until stage S6 is completed. Assumption A.2 is reasonable because new production starts from S1.

Based on the control equipment, the product can be manufactured in one cycle. The production throughput required to maintain 6 pieces of equipment/day is as follows:

$$\frac{(60 \times 8 - 28)}{3} \times \frac{1}{6} \simeq 25 \text{ (min)} \tag{14}$$

where the throughput of the previous process is set as 20 (min). In Equation (14), "28" represents the throughput of the previous process plus the idle time for synchronization. "8" is the number of processes and the total number of all processes is "8" plus the previous process. "60" is given by 20 (min) $\times$ 3 (cycles).

One process throughput (20 min) in full synchronization is

$$T_s = 3 \times 120 + 40 = 400 \text{ (min)} \tag{15}$$

Therefore, a throughput reduction of about 10% can be achieved. However, the time between processes involves some asynchronous idle time.

As a result, the above test run is as follows.

- (test run 1): Each throughput in every process (S1-S6) is asynchronous, and its process throughput is asynchronous. Table 4 represents the manufacturing time (min) in each process. Table 5 represents the variance in each process performed by workers. Table 4 represents the target time, and the theoretical throughput is given by $3 \times 199 + 2 \times 15 = 627$ (min).

  In addition, the total working time in stage S3 is 199 (min), which causes a bottleneck. Figure 26 is a graph illustrating the measurement data in Table 4,

and it represents the total working time for each worker (K1-K9). The graph in Figure 27 represents the variance data for each working time in Table 4.

- (test run 2): Set to synchronously process the throughput.

  The target time in Table 6 is 500 (min), and the theoretical throughput (not including the synchronized idle time) is 400 (min). Table 7 represents the variance data of each working process (S1-S6) for each worker (K1-K9).
- (test run 3): The process throughput is performed synchronously with the reclassification of the process. The theoretical throughput (not including the synchronized idle time) is 400 (min) in Table 8.

  Table 9 represents the variance data of Table 8. "WS" in the measurement tables represents the standard working time. This is an empirical value obtained from long-term experiments.

TABLE 4. Total manufacturing time at each stage for each worker

	WS	S1	S2	S3	S4	S5	S6
K1	15	20	20	25	20	20	20
K2	20	22	21	22	21	19	20
K3	10	20	26	25	22	22	26
K4	20	17	15	19	18	16	18
K5	15	15	20	18	16	15	15
K6	15	15	15	15	15	15	15
K7	15	20	20	30	20	21	20
K8	20	29	33	30	29	32	33
K9	15	14	14	15	14	14	14
Total	145	172	184	199	175	174	181

TABLE 5. Volatility of Table 4

K1	1.67	1.67	3.33	1.67	1.67	1.67
K2	2.33	2	2.33	2	1.33	1.67
K3	1.67	3.67	3.33	2.33	2.33	3.67
K4	0.67	0	1.33	1	0.33	1
K5	0	1.67	1	0.33	0	0
K6	0	0	0	0	0	0
K7	1.67	1.67	5	1.67	2	1.67
K8	4.67	6	5	4.67	5.67	6
K9	0.33	0.33	0	0.33	0.33	0.33

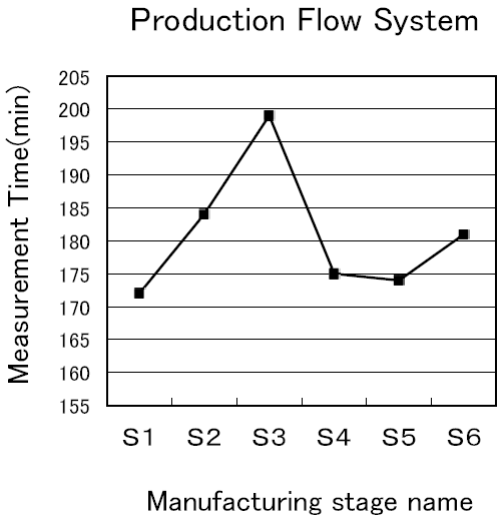

FIGURE 26. Total work time for each stage (S1-S6) in Table 4

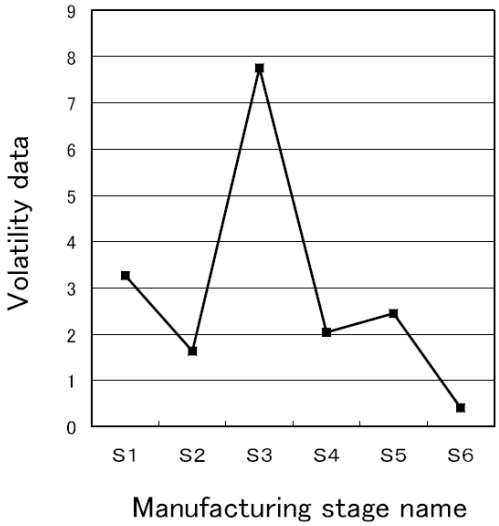

FIGURE 27. Volatility data for each stage (S1-S6) in Table 4

TABLE 6. Total manufacturing time at each stage for each worker

	WS	S1	S2	S3	S4	S5	S6
K1	20	20	(24)	20	20	20	20
K2	20	20	20	20	20	22	20
K3	20	20	20	20	20	20	20
K4	20	(25)	(25)	20	20	20	20
K5	20	20	20	20	20	20	20
K6	20	20	20	20	20	20	20
K7	20	20	20	20	20	20	20
K8	20	(27)	(27)	(22)	(23)	20	20
K9	20	20	20	20	20	20	20
Total	180	192	196	182	183	182	180

TABLE 7. Volatility of Table 6

K1	0	1.33	0	0	0	0
K2	0	0	0	0	0.67	0
K3	0	0	0	0	0	0
K4	1.67	1.67	0	0	0	0
K5	0	0	0	0	0	0
K6	0	0	0	0	0	0
K7	0	0	0	0	0	0
K8	2.33	2.33	0.67	1	0	0
K9	0	0	0	0	0	0

TABLE 8. Total manufacturing time at each stage for each worker

	WS	S1	S2	S3	S4	S5	S6
K1	20	18	19	18	20	20	20
K2	20	18	18	18	20	20	20
K3	20	(21)	(21)	(21)	20	20	20
K4	20	13	11	11	20	20	20
K5	20	16	16	17	20	20	20
K6	20	18	18	18	20	20	20
K7	20	14	14	13	20	20	20
K8	20	(22)	(22)	20	20	20	20
K9	20	(25)	(25)	(25)	20	20	20
Total	180	165	164	161	180	180	180

TABLE 9. Variance of Table 8

K1	0.67	0.33	0.67	0	0	0
K2	0.67	0.67	0.67	0	0	0
K3	0.33	0.33	0.33	0	0	0
K4	2.33	3	3	0	0	0
K5	1.33	1.33	1	0	0	0
K6	0.67	0.67	0.67	0	0	0
K7	2	2	2.33	0	0	0
K8	0.67	0.67	0	0	0	0
K9	1.67	1.67	1.67	0	0	0